Published in final edited form as:

FEBS Lett. 2023 January ; 597(1): 59–64. doi:10.1002/1873-3468.14514.

Tryptophan-96 in cytochrome P450 BM3 plays a key role in enzyme survival

Raheleh Ravanfar,

Yuling Sheng,

Harry B. Gray*, **Jay R. Winkler***

Beckman Institute, California Institute of Technology, 1200 E. California Boulevard, Pasadena, CA 91125, USA

Abstract

Flavocytochrome P450 from *Bacillus megaterium* ($P450_{BM3}$) is a natural fusion protein containing reductase and heme domains. In the presence of NADPH and dioxygen the enzyme catalyzes the hydroxylation of long-chain fatty acids. Analysis of the $P450_{BM3}$ structure reveals chains of closely spaced tryptophan and tyrosine residues that might serve as pathways for high-potential oxidizing equivalents to escape from the heme active site when substrate oxidation is not possible. Our investigations of the total number of enzyme turnovers before deactivation have revealed that replacement of selected tryptophan and tyrosine residues with redox inactive groups leads to a twofold reduction in enzyme survival time. Tryptophan-96 is critical for prolonging enzyme activity, suggesting a key protective role for this residue.

Keywords

cytochrome P450; electron transfer; tryptophan; tyrosine; total turnover number

Introduction

The cytochromes P450 (CYP) are a superfamily of heme enzymes found in archaea, bacteria, and eukaryotes that catalyze the aerobic oxidation of organic substrates [1, 2]. The CYP enzymes play critical roles both in biosynthesis and in the degradation of xenobiotic compounds. The name P450 derives from the position of the Soret absorption maximum in the ferrous-carbonmonoxy form of the enzyme. Ground and excited-state mixing of heme and cysteine thiolate orbitals accounts for the red-shifted Soret signature [3].

Decades of research have produced a consensus mechanism for CYP catalysis (Figure 1). The resting ferric enzyme is low-spin, six-coordinate, with a H_2O ligand occupying the distal axial site *trans* to the cysteine thiolate ($[(Por)(^{Cys}S)Fe^{III}(OH_2)]$). Substrate (RH) binding in the distal heme pocket induces dissociation of the aquo ligand with a concomitant conversion to high-spin and increase in the $Fe^{III/II}$ formal potential. The shift in potential enables electron transfer from NAD(P)H via a reductase, generating a

*Corresponding authors: hbgray@caltech.edu; winklerj@caltech.edu.

ferroheme that binds dioxygen to produce a ferric-superoxide heme ([(Por)(^{Cys}S)Fe^{III}(O_2^-)]$^-$). A second electron transfer, coupled with a proton transfer, leads to a ferric-hydroperoxide intermediate ([(Por)(^{Cys}S)Fe^{III}(O_2H)]$^-$). Heterolytic O—O bond cleavage produces the key intermediate, Compound I (Cmpd-I), a ferryl coupled to a ligand (porphyrin or thiolate) radical ([(Por$^•$)(^{Cys}S)Fe^{IV}(O)], [(Por)(^{Cys}S$^•$)Fe^{IV}(O)]). Cmpd-I abstracts a hydrogen atom from the substrate, generating transient Compound II ([(Por)(^{Cys}S)Fe^{IV}(OH)], Cmpd-II) and a substrate radical (R$^•$). Hydroxyl rebound from Cmpd-II back to R$^•$ produces the oxygenated product (ROH) and completes the catalytic cycle. Detours from this canonical pathway lead to uncoupling of O_2 consumption from ROH production. Loss of O_2^- from [(Por)(^{Cys}S)Fe^{III}(O_2^-)]$^-$ (autoxidation shunt), loss of H_2O_2 from [(Por)(^{Cys}S)Fe^{III}(O_2H)]$^-$ (peroxide shunt), and electron transfer to Cmpd-I (oxidase shunt) can compete with ROH production.

A longstanding curiosity about CYP enzymes is their capacity to oxygenate refractory substrates such as saturated hydrocarbons without inflicting damage on the protein or its cofactor [4, 5]. The Cmpd-I intermediate, in particular, is a powerful oxidant. If Cmpd-I forms in the absence of substrate, or in the presence of a substrate that cannot be oxygenated, how does the enzyme avoid damage? We have suggested that in this situation, electron transfer along a chain of tryptophan (Trp) and tyrosine (Tyr) residues can direct oxidizing equivalents (holes) away from the heme and toward the enzyme surface where they can be scavenged by cellular reductants [6-11].

To test this hypothesis, we have investigated catalysis in cytochrome P450$_{BM3}$ (CYP102A1), a bacterial enzyme from *Bacillus megaterium* that is a natural fusion protein of reductase and heme domains. P450$_{BM3}$ substrates are long chain fatty acids which are hydroxylated at the ω-1, ω-2, and ω-3 positions by the enzyme [12]. We have used *p*-nitrophenoxydodecanoic acid (12-*p*NCA) as a substrate because ω-1 hydroxylation produces an unstable hemiacetal that releases spectrophotometrically detectable *p*-nitrophenolate [13]. Because P450$_{BM3}$ can catalyze several hundred turnovers of 12-*p*NCA, enzyme damage must be a relatively minor pathway compared to productive catalysis. Any protective effects of Trp/Tyr chains are, therefore, unlikely to be detectable in measurements of enzyme kinetics. An enzyme protected by hole transfer along a Trp/Tyr chain, however, will complete more substrate turnovers than one lacking this pathway. Consequently, the total number of enzyme turnovers before deactivation (TTN) should be an indicator of protective pathways in catalysis. We have tested the role of Trp/Tyr chains in protecting cytochrome P450$_{BM3}$ by determining TTN values in wild-type enzymes and mutants with disrupted hole-transfer chains.

Materials and Methods

Details of substrate (12-*p*NCA) synthesis and characterization are provided in Supporting Information. All other reagents were commercially available. Full-length wild-type and mutant cytochromes P450$_{BM3}$ (CYP102A1) were expressed in *E. coli* with a C-terminal (His)$_6$ tag for isolation and purification according to published procedures [14]. Full details of expression, isolation, purification, and characterization are provided in Supporting Information.

Enzyme activity kinetics were evaluated spectrophotometrically by measuring the initial rate of of *p*-nitrophenolate appearance immediately after addition of NADPH to a solution of enzyme and 12-*p*NCA. Complete details and results are in Supporting Information. TTN values were determined by allowing the enzymes to continue oxidizing substrate, periodically removing product and adding more NADPH, until *p*-nitrophenolate production ceased. Total amount of product formed was determined spectrophotometrically. Coupling efficiency was evaluated by spectrophotometric determination of NADPH consumption.

Kinetics modeling was performed using the Matlab (The MathWorks, Inc) programming and numerical computing platform (details are in Supporting Information). Trp/Tyr hole transfer networks were identified using graph visualization tools implemented in the Bioinformatics Toolbox of the Matlab platform.

Results and Discussion

Kinetics Modeling.

We have developed a simplified model of $P450_{BM3}$ catalysis (Figure 2) to predict the effects of Trp/Tyr chain disruption on TTN values. We combine into a single step (k_F) all of the processes involved in converting [(Por)(^{Cys}S)$Fe^{III}(OH_2)$] into [(Por)(^{Cys}S)$Fe^{III}(O_2H)]^-$, implicitly assuming that the intermediate conversions are rapid and not substantially altered by Trp/Tyr mutations. We assume that two forms of Cmpd-I result from heterolytic O—O bond cleavage: the functional Cmpd-I forms with rate constant $k_{C\text{-}I}$; and a nonfunctional ferryl-ligand radical intermediate (Cmpd-I′) that forms with rate constant $k_{C\text{-}I'}$. Cmpd-I hydroxylates the substrate with rate constant k_P, but Cmpd-I′ fails to generate product, owing to the absence of substrate or the presence of a substrate that cannot be oxygenated. We propose that Cmpd-I′ leads to deactivated enzyme (k_D) but can be rescued by hole transfer away from the heme (k_R). We also assume that the rescue pathway can direct holes away from the functional Cmpd-I intermediate with the same rate constant (k_R). A peroxide shunt pathway also is included (k_H) to model the uncoupling reactions. Although this is an extremely simplified version of P450 catalysis, the rate law is still too complex to solve analytically. We can, however, develop an expression for TTN and coupling efficiency by considering the relative yields of the three branches originating from [(Por)(^{Cys}S)$Fe^{III}(O_2H)]^-$.

$$\mathrm{TTN} = \frac{\phi_{\mathrm{ROH}}}{\phi_{\mathrm{DEAD}}} = \frac{\phi_{\mathrm{C-I}}\phi_{k_P}}{\phi_{\mathrm{C-I'}}\phi_{\mathrm{D}}} = R_{\mathrm{C-I}}\frac{(1+R_{\mathrm{D}})}{(1+R_{\mathrm{P}})} \approx R_{\mathrm{C-I}}(1+R_{\mathrm{D}}) \quad (1)$$

TTN will be given by the relative yields of ROH production and enzyme death (eq. 1). In this approximation, TTN depends on the ratio of Cmpd-I and Cmpd-I′ formation rate constants ($R_{C\text{-}I} = k_{C\text{-}I}/k_{C\text{-}I'}$), the ratio of rate constants for rescue and damage ($R_D = k_R/k_D$), and the ratio of rate constants for rescue and product formation ($R_P = k_R/k_P$). If the rescue pathway does not compete with product formation (i.e., $R_P \ll 1$), then TTN is approximately equal to $R_{C\text{-}I}(1 + R_D)$. The efficiency of coupling ROH production to O_2

$$\text{Coupling} = \frac{1}{\left(1 + \frac{1}{R_{C-I}} + R_H\right)(1 + R_P)} \approx \frac{1}{\left(1 + \frac{1}{R_{C-I}} + R_H\right)} \quad (2)$$

consumption depends on the same parameters as well as the ratio of rate constants for H_2O_2 production and Cmpd-I formation ($R_H = k_H/k_{C\text{-}I}$) (eq. 2).

The critical parameter for enzyme protection in this model is k_R, the rate constant for delivery of holes away from Cmpd-I′. Using semiclassical electron transfer (ET) theory and the structure of the $P450_{BM3}$ heme domain (PDB ID 2IJ2) [15], we can estimate the survival time of a high-potential hole at the heme in wild-type and mutants of $P450_{BM3}$. Details of the rate calculations are in Supporting Information. Analysis of Tyr/Trp hole transfer pathways from the $P450_{BM3}$ heme with a 10-Å cutoff for maximum ET distance reveals a direct pathway from the heme through W96 to surface exposed residues W90 and Y334 (Figure 3A). Relaxing the distance constraint to 15 Å exposes the possible involvement of many more residues and pathways (Figure 3B). W96, the closest Trp or Tyr residue to the heme, is a likely gateway for hole transfer from the heme. Y115 is the next closest redox-active residue, but kinetics simulations do not predict a substantial enhancement of heme hole survival over the W96H mutant. Calculations indicate that residues W325 and Y256, each 12.8 Å from the heme, would accept holes if W96 were unavailable. We estimated heme hole survival times for wild-type and four mutants (W96H, W96H/W90F, W96H/W90F/Y334F, W96H/Y256F/W325F; see Supporting Information) (Figure 4). Removal of W96 from the hole transfer pathway is expected to protract the lifetime of a hole on the heme by about a factor of 8. Replacement of additional residues in the W96-W90-Y334 pathway has only a modest impact. An additional fourfold increase in heme hole lifetime is estimated for the W96H/Y256F/W325F triple mutant.

Enzyme Activity.

We evaluated the activity of wild-type and mutant $P450_{BM3}$ by determining the initial rates of *p*-nitrophenolate production as functions of 12-*p*NCA concentration (2-128 μM). All enzymes exhibited rate saturation at [12-*p*NCA] > 60 μM (Supporting Information). Fits of the data to a Michaelis-Menten kinetics model produced k_{cat} and K_M values that varied by about a factor of 2.5 among the different enzymes, although the enzyme activities defined by k_{cat}/K_M remained relatively constant (Table 1). The mutations tended to lower the maximum turnover rate compared to the wild-type enzyme with the largest decrease appearing in the W96H/W90F mutant. The K_M values were lower in the mutants, suggesting somewhat tighter substrate binding. Care should be taken when interpreting these parameters, as the complex P450 mechanism (Figure 1) is a far cry from the ideal Michaelis-Menten model.

Total turnover numbers.

We allowed the wild-type and mutant enzymes to react with substrate, periodically removing product and replenishing NADPH and substrate, until consumption of NADPH ceased. At the termination of catalysis, the amount of *p*-nitrophenolate produced was determined spectrophotometrically and divided by the amount of enzyme to give TTN values (Figure 5, Table 2). On average, each wild-type enzyme converts $(3.4\pm0.2)\times10^2$ substrate molecules

before deactivation. The mutant protein TTN values are roughly comparable to one another, in the range of 48-70% of wild-type TTN.

These observations are broadly consistent with predictions of the kinetics modeling. The W96H mutation is expected to have the largest impact on k_R, lowering the R_D ratio, and reducing the TTN value. The W90F and Y334F mutations are not predicted to lower k_R substantially, and we observe only modest further reductions in TTN. The W96H/Y256F/W325F enzyme is expected to have a fourfold smaller k_R value, but its TTN value is close to that of the W96F mutant. This observation suggests that the decrease in k_R resulting from the W96H mutation leads to $R_D \ll 1$, so that further reductions in k_R have little impact on TTN.

The kinetics model suggests that the coupling efficiency should not be greatly affected by changes in k_R (eq. 2). Our observation that coupling efficiencies decreased in the mutant proteins (Table 1) may indicate that the kinetics of the peroxide shunt (k_H) and/or the autoxidation pathways (not included explicitly in our model) may not be the same for all P450s in our study.

Concluding Remarks

Replacement of selected Trp and Tyr residues in the heme domain of cytochrome $P450_{BM3}$ negatively impacts enzyme survival. A possible explanation for this behavior is that the Trp and Tyr residues are members of a hole transfer chain that deliver potentially damaging oxidizing equivalents away from the heme when substrate oxidation is prevented. Our simplified model of $P450_{BM3}$ catalysis and protection is consistent with our observations of total turnover numbers in wild-type and mutant enzymes. W96 appears to be the gateway residue for the primary Trp/Tyr protection pathway. Sequence alignments suggest that this position is more commonly occupied by a histidine residue in bacterial enzymes, but tryptophan is found at this position in more than 80% of mammalian P450s [16]. High enzyme turnover rates have been associated with increased energy demand and reduced productivity in microbes and plants [17, 18]. In the case of $P450_{BM3}$ it is difficult to assess whether the twofold increase in enzyme turnover resulting from the placement of a tryptophan residue at position 96 offers a substantial selective advantage to the organism. Full-length cytochrome $P450_{BM3}$ is relatively large and a conservative estimate suggests that more than 4700 ATP molecules are required to degrade and resynthesize one enzyme [19]. This energetic cost may be great enough to provide a selective advantage for a wild-type enzyme that functions two times longer than a single site variant (e.g., W96H).

Supplementary Material

Refer to Web version on PubMed Central for supplementary material.

Acknowledgements

This research was supported by the National Institute of Diabetes and Digestive and Kidney Diseases of the National Institutes of Health under Award Number R01DK019038. The content is solely the responsibility of the authors and does not necessarily represent the official views of the National Institutes of Health. Additional support was provided by the Arnold and Mabel Beckman Foundation.

Data Availability

The data that support the findings of this study are available in Table 1, Table 2, Figure 4, Figure 5, and the supplementary material of this article.

Abbreviations:

$P450_{BM3}$	flavocytochrome P450 from *Bacillus megaterium*
Cmpd-I	cytochrome P450 Compound I
Cmpd-II	cytochrome P450 Compound II
12-*p*NCA	*p*-nitrophenoxydodecanoic acid
Trp	tryptophan
Tyr	tyrosine
TTN	total turnover number

References

1. Denisov IG, Makris TM, Sligar SG & Schlichting I (2005) Structure and chemistry of cytochrome P450, Chem Rev. 105, 2253–2277. [PubMed: 15941214]
2. Ortiz de Montellano PR (2015) Cytochrome P450 - Structure, Mechanism, and Biochemistry, Springer, Switzerland.
3. Hanson LK, Eaton WA, Sligar SG, Gunsalus IC, Gouterman M & Connell CR (1976) Origin of the anomalous Soret spectra of carboxycytochrome P-450, J Am Chem Soc. 98, 2672–2674. [PubMed: 1262660]
4. Green MT, Dawson JH & Gray HB (2004) Oxoiron(IV) in Chloroperoxidase Compound II is Basic: Implications for P450 Chemistry, Science. 304, 1653–1656. [PubMed: 15192224]
5. Groves JT (2003) The bioinorganic chemistry of iron in oxygenases and supramolecular assemblies, Proc Natl Acad Sci USA. 100, 3569–3574. [PubMed: 12655056]
6. Gray HB & Winkler JR (2015) Hole hopping through tyrosine/tryptophan chains protects proteins from oxidative damage, Proc Natl Acad Sci USA. 112, 10920–10925. [PubMed: 26195784]
7. Gray HB & Winkler JR (2016) The Rise of Radicals in Bioinorganic Chemistry, Isr J Chem. 56, 640–648. [PubMed: 28239191]
8. Gray HB & Winkler JR (2018) Living with Oxygen, Acc Chem Res. 51, 1850–1857. [PubMed: 30016077]
9. Gray HB & Winkler JR (2021) Functional and protective hole hopping in metalloenzymes, Chem Sci. 12, 13988–14003. [PubMed: 34760183]
10. Winkler JR & Gray HB (2015) Could tyrosine and tryptophan serve multiple roles in biological redox processes?, Phil Trans R Soc A. 373.
11. Winkler JR & Gray HB (2015) Electron flow through biological molecules: does hole hopping protect proteins from oxidative damage?, Quart Rev Biophys. 48, 411–420.
12. Warman AJ, Roitel O, Neeli R, Girvan HM, Seward HE, Murray SA, McLean KJ, Joyce MG, Toogood H, Holt RA, Leys D, Scrutton NS & Munro AW (2005) Flavocytochrome P450BM3: an update on structure and mechanism of a biotechnologically important enzyme, Biochem Soc Trans. 33, 747–753. [PubMed: 16042591]
13. Schwaneberg U, Schmidt-Dannert C, Schmitt J & Schmid RD (1999) A Continuous Spectrophotometric Assay for P450 BM-3, a Fatty Acid Hydroxylating Enzyme, and Its Mutant F87A, Anal Biochem. 269, 359–366. [PubMed: 10222011]

14. Wang ZJ, Renata H, Peck NE, Farwell CC, Coelho PS & Arnold FH (2014) Improved Cyclopropanation Activity of Histidine-Ligated Cytochrome P450 Enables the Enantioselective Formal Synthesis of Levomilnacipran, Angew Chem, Int Ed. 53, 6810–6813.

15. Girvan HM, Seward HE, Toogood HS, Cheesman MR, Leys D & Munro AW (2007) Structural and spectroscopic characterization of P450BM3 mutants with unprecedented P450 heme iron ligand sets - New heme ligation states influence conformational equilibria in P450BM3, J Biol Chem. 282, 564–572. [PubMed: 17077084]

16. Sørensen MLH, Sanders BC, Hicks LP, Rasmussen MH, Vishart AL, Kongsted J, Winkler JR, Gray HB & Hansen T (2020) Hole Hopping through Cytochrome P450, The Journal of Physical Chemistry B. 124, 3065–3073. [PubMed: 32175746]

17. Hanson AD, McCarty DR, Henry CS, Xian X, Joshi J, Patterson JA, García-García JD, Fleischmann SD, Tivendale ND & Millar AH (2021) The number of catalytic cycles in an enzyme's lifetime and why it matters to metabolic engineering, Proc Natl Acad Sci USA. 118, e2023348118. [PubMed: 33753504]

18. Koehn RK (2008) The cost of enzyme synthesis in the genetics of energy balance and physiological performance, Biological Journal of the Linnean Society. 44, 231–247.

19. Lahtvee P-J, Seiman A, Arike L, Adamberg K & Vilu R (2014) Protein turnover forms one of the highest maintenance costs in Lactococcus lactis, Microbiology. 160, 1501–1512. [PubMed: 24739216]

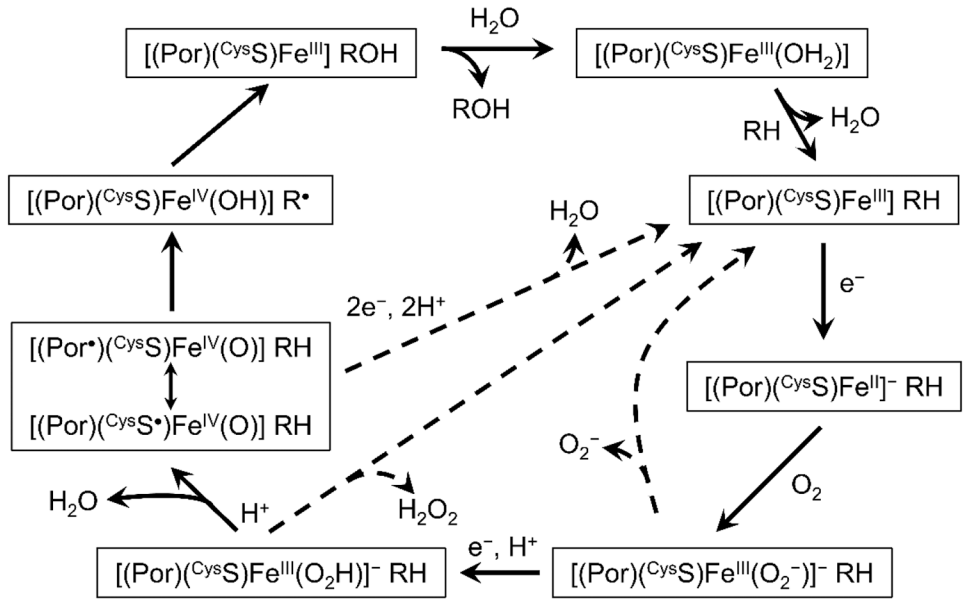

Figure 1.
Consensus mechanism for cytochrome P450 catalysis. Dashed arrows indicate uncoupling pathways.

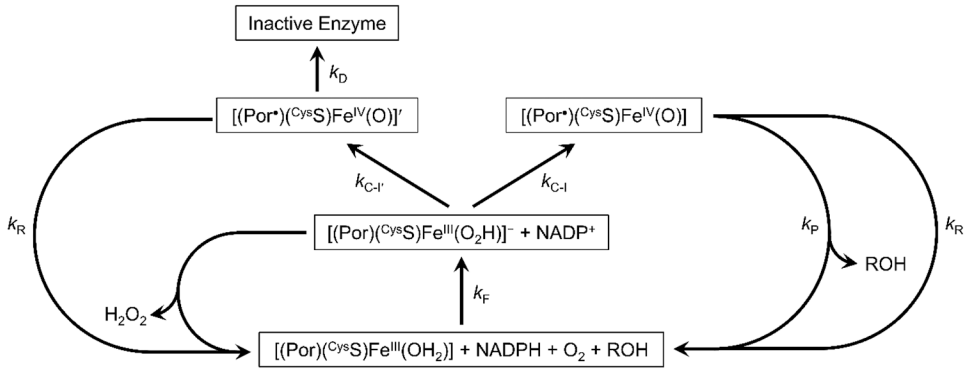

Figure 2.

Simplified kinetics model of cytochrome $P450_{BM3}$ catalysis, uncoupling, and inactivation.

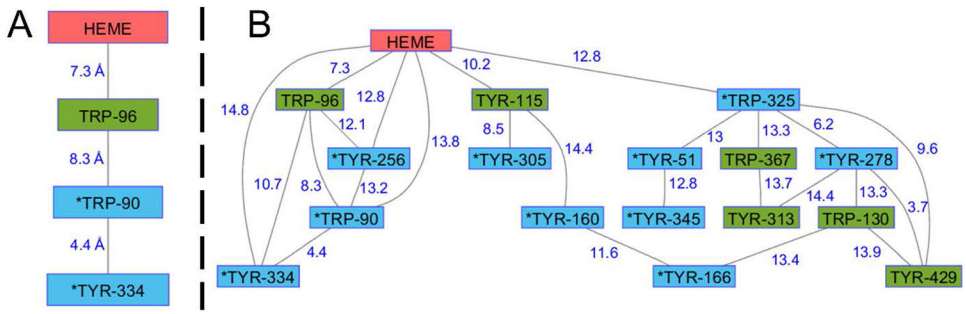

Figure 3.

Trp/Tyr hole transfer networks in $P450_{BM3}$. (A) 10-Å ET distance cutoff. (b) 15-Å ET distance cutoff. Asterisks denote surface-exposed residues.

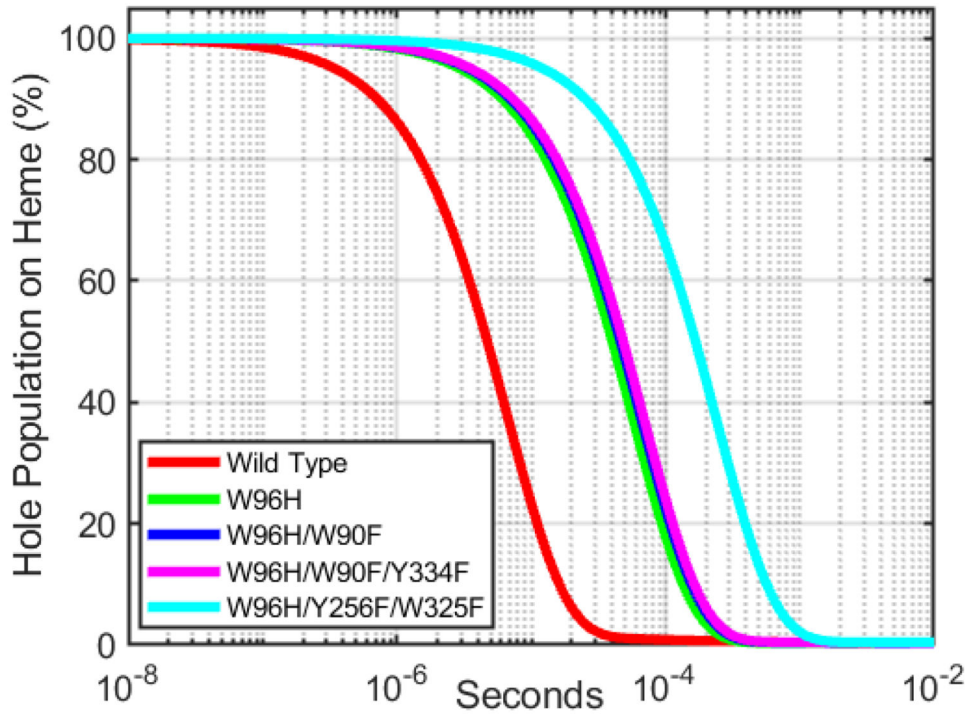

Figure 4.
Predicted heme-hole survival kinetics in wild-type and mutant cytochromes $P450_{BM3}$.

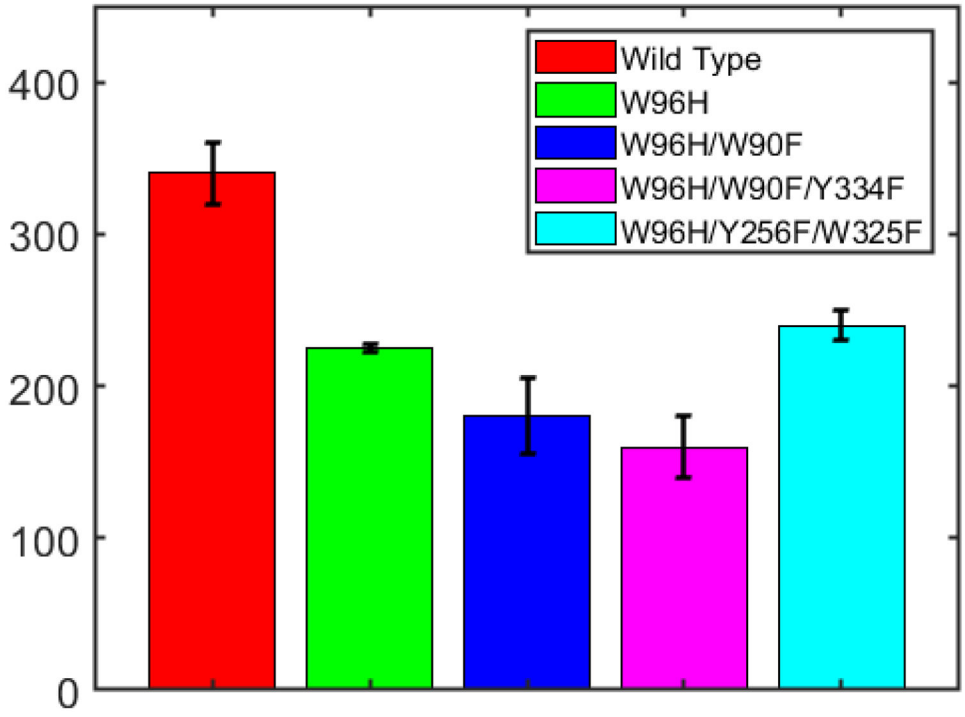

Figure 5.
TTN values for wild-type and W96H, W96H/W90F, W98H/W90F/Y334F, and W96H/Y256F/W325F mutants of cytochrome $P450_{BM3}$.

Table 1.

Parameters extracted from wild-type and mutant cytochrome $P450_{BM3}$ kinetics measurements.

	Wild-type	W96H	W96H/W90F	W96H/W90F/Y334F	W96H/W256F/Y325F
k_{cat} (s^{-1})	1.8±0.3	1.7±0.1	0.7±0.1	1.45±0.3	1.2±0.2
K_M (μM)	22±9	17.5±4.0	9±2	14.±4	9±4
k_{cat}/K_M ($M^{-1}s^{-1}$)	$(9.1\pm2)\times10^4$	$(1.0\pm0.2)\times10^5$	$(8.2\pm2)\times10^4$	$(1.1\pm0.2)\times10^5$	$(1.4\pm0.4)\times10^5$

Table 2.

TTN values and coupling efficiencies for wild-type and mutant cytochromes $P450_{BM3}$.

	Wild-type	W96H	W96H/W90F	W96H/W90F/Y334F	W96H/W256F/Y325F
TTN	$(3.4\pm0.2)\times10^2$	$(2.25\pm0.03)\times10^2$	$(1.8\pm0.25)\times10^2$	$(1.6\pm0.2)\times10^2$	$(2.4\pm0.1)\times10^2$
Coupling (%)	12.1±0.1	8.9±2.2	9.1±0.9	9.9±1.2	8.9±1.3